



Cite this: *Chem. Commun.*, 2021, 57, 3496

Received 25th January 2021,
 Accepted 28th February 2021

DOI: 10.1039/d1cc00429h

rsc.li/chemcomm

Construction and theoretical insights into the ESIPT fluorescent probe for imaging formaldehyde *in vitro* and *in vivo*†

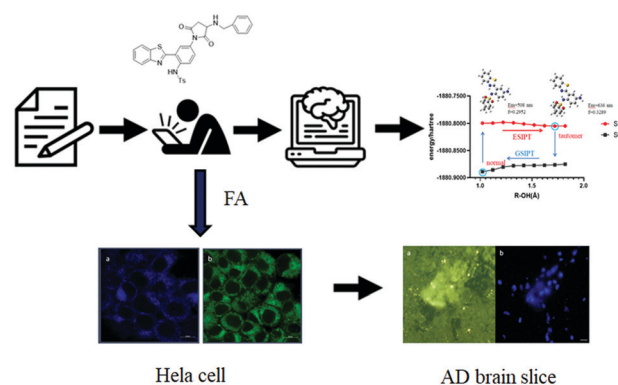
Anyao Bi,^{ab} Min Liu,^{ab} Shuai Huang,^{ab} Fan Zheng,^{ab} Jipeng Ding,^{ab} Junyong Wu,^c Gao Tang^{ab} and Wenbin Zeng^{ib} *^{ab}

We report the first ESIPT-based probe ABTB, for the highly sensitive and selective imaging of formaldehyde (FA). The various theoretical calculations have been systematically performed, and clearly unravel the lighting mechanism of the fluorescent probe for FA. Additionally, the probe was successfully applied in monitoring endogenous FA in the brain of AD mice.

Formaldehyde (FA, HCHO), the simplest aldehyde, is widely used in many industrial productions such as cosmetics, plastic products and pharmaceuticals. It is a colourless, carcinogenic and mutagenic organic contaminant with a strong odor.¹ The World Health Organization (WHO) and the US Environmental Protection Agency (EPA) have identified HCHO as the first class of carcinogenic and teratogenic substances. Indoor air, the atmospheric environment and food contamination caused by formaldehyde can give rise to memory damage, dizziness, headaches, nausea, and even death.^{2–5} In living organisms, under the catalysis of demethylase or oxidase, formaldehyde may also be produced in metabolic processes such as methylation of DNA or demethylation of histones.^{6,7} FA presents in almost all cells and plays an important role in the carbon cycle metabolism process.^{8,9} In addition, normal levels of formaldehyde are closely related to spatial memory and cognitive ability.^{10,11} It is not difficult to find that FA is closely related to our lives; both daily life and our physical health. Therefore, the development of an effective fluorescent probe for tracking and monitoring FA in biological systems is important and urgently required.

At present, FA detection methods mainly include fluorescence spectrophotometry, chromatography, electrochemical sensing *etc.*¹² However, chromatography has inadequacies of poor qualitative ability and complicated operation. Fluorescence spectrophotometry presents high sensitivity and quantitative analysis, but it has some defects too. For example, it is easily interfered with by ions, the fluorescence is not concentrated, and the fluorescence intensity is not high. Electrochemical sensing has good repeatability, accuracy and resolution, but it has the disadvantages of high detection cost, long operation time and complicated sample processing. These shortcomings of the above methods inhibit their further application. Thus, it is necessary to develop an efficient detection method with simple operation, high sensitivity and low cost (Scheme 1).

In recent years, fluorescent probes have become powerful and effective tools for biological detection due to their simplicity, low detection limit, high specific selectivity, real-time detection, and good biocompatibility.¹³ However, to date, only a small number of fluorescent probes for detecting formaldehyde have been



Scheme 1 Schematic illustration of construction and theoretical insight studies with the ESIPT fluorescent probe for FA detection in cells and the AD brain model.

^a Xiangya School of Pharmaceutical Sciences, Central South University, Changsha, 410013, P. R. China. E-mail: wbzeng@hotmail.com, wbzeng@csu.edu.cn; Fax: +86-731-82650459; Tel: +86-731-82650459

^b Hunan Key Laboratory of Diagnostic and Therapeutic Drug Research for Chronic Diseases, Changsha 410078, China

^c Department of Pharmacy, the Second Xiangya Hospital, Central South University, Changsha, 410011, China

† Electronic supplementary information (ESI) available: Experimental details and supplementary figures. See DOI: 10.1039/d1cc00429h

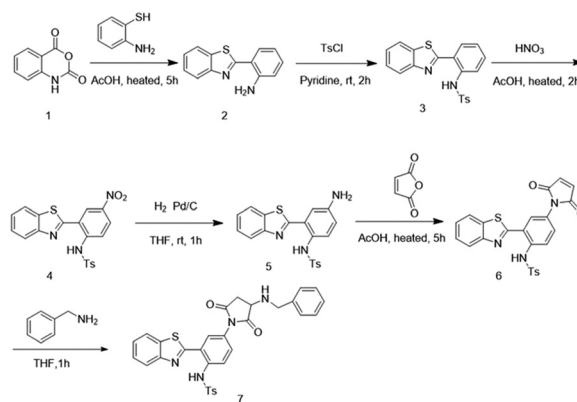
developed. There are two main types of reaction-based fluorescent probes for detecting FA that have been reported so far. One is a Schiff reactivity-based small molecular fluorescent probe. In 2017, our group designed and synthesized a novel fluorescent probe (**MPAD**) for quantitative determination of formaldehyde (0–50 μM) with an ultra-fast detection time (6 min) and an ultra-low detection limit (20 nM). The fluorescence of the probe dramatically enhanced in aqueous solution with the addition of FA based on the photo induced electron transfer (PET) process.¹⁴ In 2018, Wang's group reported two kinds of graceful FA regenerative fluorescent probes for the first time. The fluorescence-initiated response was based on a unique dual PET/ICT quenching mechanism, thereby achieving regional-specific detection of FA.¹⁵ Compared with the off-on fluorescent probes, ratiometric-type probes have the ability to eliminate background interference in the analysis process.

The excited state intramolecular proton transfer (ESIPT), fluorescence resonance energy transfer (FRET), and intramolecular charge transfer (ICT) processes, are important mechanisms for constructing ratiometric fluorescent probes. In particular, ESIPT has received considerable attention due to its dual emission behaviour,¹⁶ large Stokes shifts, and environmentally sensitive emission profile.¹⁷ In sharp contrast to the multitude of papers reporting hydroxyl-type ESIPT, only a few reports have dealt with amino-type ESIPT.¹⁸ Compared with the hydroxyl-type ESIPT, amino-type ESIPT uses primary amines as proton donors due to their good photostability. Increasing experimental interest has been devoted to fluorophore molecular design to achieve optimal optical properties. However, there are few efforts towards fundamental mechanistic studies.

In this paper, we in-sighted the fluorescence mechanism in the ESIPT systems of the **ABTB** probe with ideal quantum chemical tools. These studies went beyond the common strategy of analysing frontier orbital energy diagrams and performing ESIPT thermodynamics calculations. Instead, the potential energy surfaces (PES) of the lowest-lying excited states are explored with time-dependent density functional theory (TD-DFT). So far, no fluorescent probe has been applied in monitoring dynamic changes of endogenous FA in AD live brains. Herein, we report the first ESIPT fluorescent probe **ABTB**, to visualize endogenous formaldehyde in the pathological processes of AD live brains (Scheme 2).

To understand the emission mechanism of these fluorophores it is essential to design and construct a fluorescent probe. The fluorophore **ABT** of FA probe **ABTB**, and FA reaction probe product **ABTBF**, were researched first. Starting from the S1-state ESIPT structure of enol, we simulated and scanned possible configurations with its excited-state energy, and explored the S1-profile *via* a series of constrained geometry optimizations, including the N–H distances of solvated **ABT**. Starting from the enol structure, the solvent coordinates *via* the ESIPT process from about an N–H distance, creating keto*. The PBE0/def2-SVP optimized **ABT**, are shown in Fig. 1. The computational results indicate that in the DMSO solution, once excited to the S1 state, the molecule tends to undergo an ESIPT transformation from an enol to keto tautomer.

At the PBE0 level, our calculations started in the S0 state from enol, possible configurations of **ABT** including keto, are



Scheme 2 Synthesis of fluorescent probe **ABTB**.

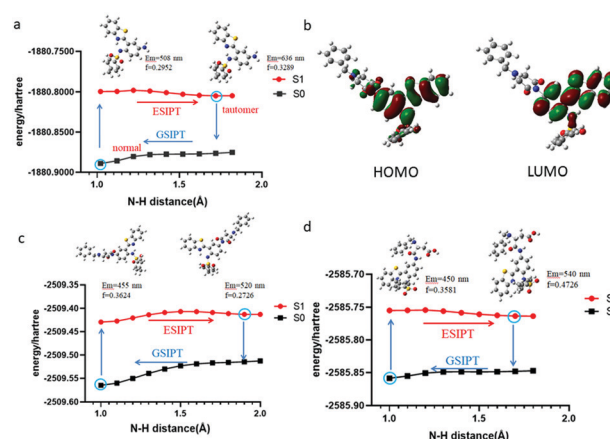


Fig. 1 (a) The **ABT** (PBE0/def2-SVP)-optimized S1 energy profiles along the N–H distances. (b) The molecular orbitals (LUMO and HOMO) of **ABTB**. (c) The **ABTB** (PBE0/def2-SVP)-optimized S1 energy profiles along the N–H distances. (d) The **ABTBF** (PBE0/def2-SVP)-optimized S1 energy profiles along the N–H distances.

also summarized in Fig. 1a. Then the vertical excitation energy was calculated at enol to predict its fluorophore spectra. The S0 \rightarrow S1 excitation shows a spectroscopically bright state with π – π^* character, which mainly results from the HOMO to LUMO excitation. The S0 \rightarrow S1 vertical excitation energy calculated by TD-PBE0 with def2-SVP approach is 350 nm. Both of these results are close to the experimentally measured absorption maximum of 365 nm. The FA reaction probe product **ABTBF**, keto*, shows a vertical emission energy of 540 nm ($f = 0.4726$) at the TD-PBE0 level, with the def2-SVP approach, which is in excellent agreement with the experimental fluorescence emission of 525 nm; therefore, keto* is assigned as the most likely emissive structure on the S1 state. In short, using the TD-PBE0/def2-SVP approach in combination with electronic-structure calculations, we have comprehensively sighted the emission channels of **ABT** and **ABTBF**, thus confirming that fluorescence emission is contributed by ESIPT.

With **ABTB** in hand, the photophysical properties and sensing abilities of the probe towards FA were investigated. As shown in

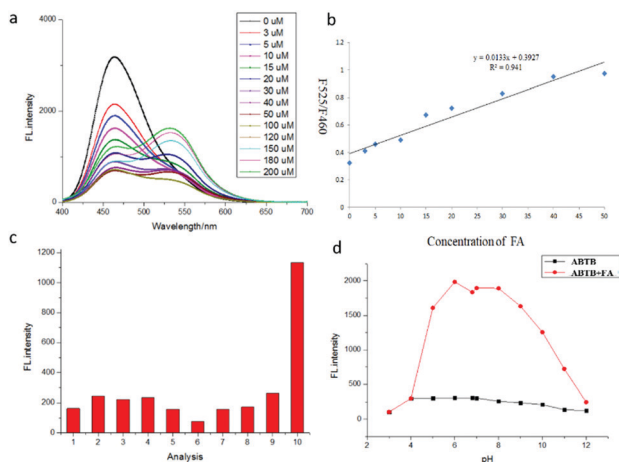


Fig. 2 (a) The fluorescence intensity of **ABTB** (10 μM) was recorded after addition of formaldehyde in aqueous solution, (b) linear relationship between $I_{460\text{ nm}}/I_{525\text{ nm}}$ of **ABTB**, (c) the fluorescence intensity of **ABTB** (10 μM) with various relevant analytes in PBS. (1. Benzaldehyde, 2. acetaldehyde, 3. propionaldehyde, 4. methyl formate, 5. ethyl formate, 6. glyoxal, 7. acetone, 8. acetic acid, 9. furfural, 10. formaldehyde.) (d) pH investigation for sensing FA with **ABTB**.

Fig. 2a, we recorded the fluorescence intensity of **ABTB** in the presence of different concentrations of formaldehyde in aqueous solution. After adding an increased concentration of formaldehyde, it showed a distinct spectral change. The fluorescence intensity of the probe at 460 nm decreased with the addition of FA, while the fluorescence intensity of the new emission peak at 525 nm gradually increased. In addition, the linear response of $I_{460\text{ nm}}/I_{525\text{ nm}}$ to formaldehyde was also investigated (Fig. 2b). As shown in Fig. 2b, the fluorescence intensity ratio of the probe ($I_{460\text{ nm}}/I_{525\text{ nm}}$) was linearly related to the concentration of formaldehyde (0–50 μM). The results indicated that probe **ABTB** was capable of detecting FA quantitatively in ratio, and it can fully meet the requirements of formaldehyde detection in the environment as well. To evaluate the selectivity of **ABTB** towards FA, we selected a variety of common small molecule aldehyde-containing compounds to make a comparison, including benzaldehyde, acetaldehyde, propionaldehyde, methyl formate, ethyl formate, glyoxal, acetone, acetic acid, furfural and formaldehyde. It was found that probe **ABTB** only showed significant fluorescence enhancement at 525 nm for formaldehyde, and weak fluorescence changes for other tested small molecules (Fig. 2c). It was confirmed that probe **ABTB** has excellent selectivity to formaldehyde.

In addition, the suitable pH range for FA sensing was also investigated (Fig. 2d). As shown in Fig. 2d, the fluorescence intensity was stable in the range pH 3 to 12. While **ABTB** was reacted with FA, the fluorescence intensity of the system was the largest and almost constant in the range of pH 6–8, while the fluorescence intensity gradually decreased at pH < 6 or pH > 8. Therefore, probe **ABTB** has a good response to FA under physiological pH conditions, and could achieve high sensitivity fluorescence detection of formaldehyde in acidic and neutral aqueous solutions. These results provided favourable conditions for the detection of the fluorescent probe in a complex environment.

The response mechanism of **ABTB** towards FA was further discussed. **ABTB** was developed as a reaction-based fluorescent probe for FA detection *via* a new type mechanism with concurrent release of total FA after detection. In the absence of FA, the fluorescent intensity of **ABTB** at 525 nm was so weak because of PET and ICT quenching pathways. Upon reaction with FA, the lone pair electrons in nitrogen attacked the carbon on FA, transforming secondary nitrogen into tertiary nitrogen. Hydroxyl attacked the carbonyl carbon which was linked to nitrogen, resulting in the cleavage of the five-membered heterocycle and the formation of six-membered azalactone. This convention contributed to the removal of ICT; however, **ABTB** still failed to emit fluorescence because of PET quenching from the electron-rich amino substituents. After 2-aza-Cope rearrangement in aqueous solution, its structure was further changed through the breaking of the ester bond while the PET quenching effect still existed. However, the instability of the chemical structure would cause the C–N bond to break. The structural change resulted in a turn-on emission by the removal of PET, with concomitant release of the captured FA caused by the C–N bond breaking. Therefore, FA consumption-free detection is achieved.

The proposed detection mechanism was then confirmed by HPLC-MS analysis. We first incubated **ABTB** (10 nmol) with 5 equiv. FA (50 nmol) in aqueous solution with the addition of 3 mL THF for 5 h. After filtering through a syringe, the solution was tested by HPLC-MS. As displayed in Fig. 3, **ABTB** ($t = 6.5\text{ min}$) was gradually consumed while a new fluorescent product ($t = 5.5\text{ min}$) was generated. The chemical structure of the new product was confirmed to be product ($M_r = 600.15$) by mass spectrometry ($m/z = 601.1574$, see ESI[†]). The results entirely corresponded with our expectations, thereby proving the predicted mechanism.

With the above findings, we then investigated the imaging ability of **ABTB** with HCHO in living cells. In the control experiment, HeLa cells were only incubated for 30 min with the probe (10 μM) (Fig. 4a). The distinct blue fluorescence of **ABTB** appeared mainly in the cytoplasm. We further evaluated the change of fluorescence upon the addition of FA in cells. After 30 min incubation with the probe, HeLa cells were then incubated with HCHO (20 mM) for another 30 min. Only green fluorescence showed up rather than the blue fluorescence

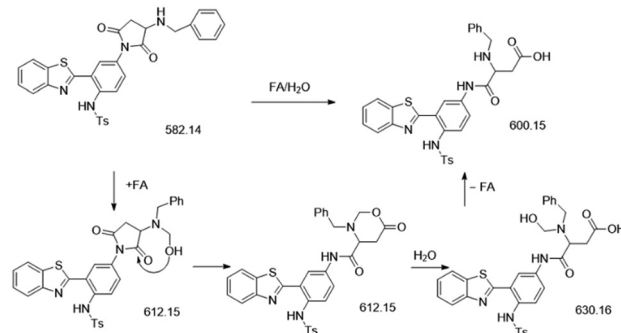


Fig. 3 The proposed mechanism of the reaction of **ABTB** and FA by MS.

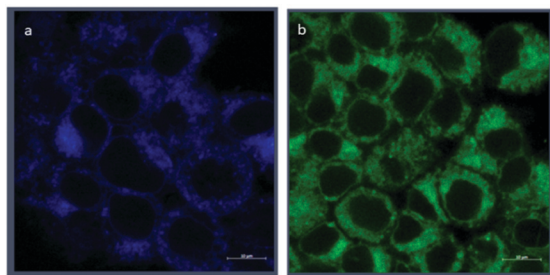


Fig. 4 Confocal fluorescence imaging for FA detection in living HeLa cells using **ABTB**. (a) Fluorescence images of HeLa cells incubated with **ABTB** (10 μ M) for 30 min (control); (b) fluorescence images of HeLa cells incubated with **ABTB** (10 μ M) for 30 min and then incubated with FA (20 mM) for 30 min; scale bars, 10 μ m.

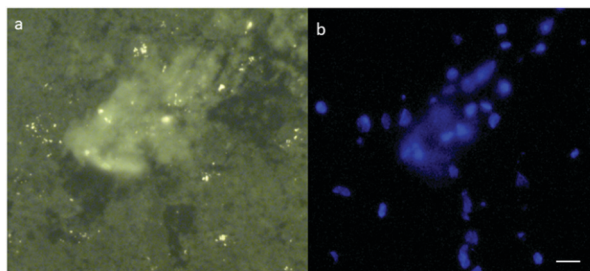


Fig. 5 Brain tissue section stained using **ABTB** (a: green light) and DAPI (b: blue light) in the brain of an AD mouse model. Scale bars, 50 μ m.

arising from **ABTB**. These results revealed that the probe has good staining capability towards FA in living cells.

The imaging suitability of **ABTB** towards FA was further assessed in the live animal brain, especially in AD brains. Our previous work constructed a mouse brain model for glioma imaging.¹⁹ Here, an AD mouse model was successfully screened and established with C57. The brain tissue section was then obtained. After **ABTB** addition, an obvious yellow fluorescence was observed in the AD brain tissue section. In addition, the imaging region by **ABTB** was consistent with the blue fluorescence by DAPI staining. These results indicate that **ABTB** has great potential to monitor endogenous formaldehyde in the pathological processes of AD live brains (Fig. 5).

In summary, **ABTB** is the first ESIPT fluorescent probe for imaging endogenous FA in cells and in live AD mice brain tissues. With the probe, only blue fluorescence showed up in HeLa cells, while it changed into green fluorescence after incubation with FA. The lighting mechanism of the fluorescent probe for formaldehyde was clearly unravelled through systematic theoretical calculations. The imaging ability of **ABTB** with HCHO was further proved in the AD mouse model. This work provides a

robust chemical tool for the detection of endogenous FA *in vivo* and might have potential applications in the diagnosis of FA-related neurodegenerative diseases.

This work was supported by the financial support from the National Natural Science Foundation of China (81971678 and 81671756), the Science and Technology Foundation of Hunan Province (2020SK3019, 2019SK2211 and 2019GK5012), and the Innovation Fund for Postgraduate Students of Central South University (2019zzts770), and the Fundamental Research Funds for the Central Universities of Central South University (2018zzts041, 2018dcyj067).

Conflicts of interest

The authors declare no competing financial interest.

Notes and references

- 1 T. Salthammer, S. Mentese and R. Marutzky, *Chem. Rev.*, 2010, **110**, 2536.
- 2 A. Lino-dos-Santos-Franco, H. V. Domingos, A. P. L. de Oliveira, A. C. Breithaupt-Faloppa, J. P. S. Peron, S. Bolonheis, M. N. Muscará, R. M. Oliveira-Filho, B. B. Vargaftig and W. Tavares-de-Lima, *Toxicol. Lett.*, 2010, **197**, 211.
- 3 B. Killhovd, A. Juutilainen, S. Lehto, T. Rönnemaa, P. Torjesen, K. F. Hanssen and M. Laakso, *Atherosclerosis*, 2009, **205**, 590.
- 4 Z. Tong, W. Luo, Y. Wang, F. Yang, Y. Han, H. Li, H. Luo, B. Duan, T. Xu, Q. Maoying, H. Tan, J. Wang, H. Zhao, F. Liu and Y. Wan, *PLoS One*, 2010, **5**, e10234.
- 5 K. Wang, W. Ma, Y. Xu, X. Liu, G. Chen, M. Yu, Q. Pan, C. Huang, X. Li, Q. Mu, Y. Sun and Z. Yu, *Chin. Chem. Lett.*, 2020, **12**, 3149.
- 6 D. Wu, D. Wang, X. Ye, K. Yuan, Y. Xie, B. Li, C. Huang, T. Kuang, Z. Yu and Z. Chen, *Chin. Chem. Lett.*, 2020, **6**, 1504.
- 7 S. Sun, Q. Guan, Y. Liu, B. Wei, Y. Yang and Z. Yu, *Chin. Chem. Lett.*, 2019, **5**, 1051.
- 8 X. Weng, C. H. Chon, H. Jiang and D. Li, *Food Chem.*, 2009, **114**, 1079.
- 9 Y. Liu, Y. Yuan, X. Lei, H. Yang, S. A. Ibrahim and W. Huang, *Food Chem.*, 2013, **138**, 2174.
- 10 Y. Liu, Z. Ye, H. Yang, L. Zhou, D. Fan, S. He and D. Chui, *Neuroscience*, 2010, **169**, 1248.
- 11 K. Tulpule and R. Dringen, *J. Neurochem.*, 2013, **127**, 7.
- 12 K. Kawamura, K. Kerman, M. Fujihara, N. Nagatani, T. Hashiba and E. Tamiya, *Sens. Actuators, B*, 2005, **105**, 495.
- 13 H. Zheng, X. Q. Zhan, Q. N. Bian and X. J. Zhang, *Chem. Commun.*, 2013, **49**, 429.
- 14 A. Bi, T. Gao, X. Cao, J. Dong, M. Liu, N. Ding, W. Liao and W. Zeng, *Sens. Actuators, B*, 2018, **255**, 3292.
- 15 H. Xu, S. Ma, Q. Liu, L. Huang, P. Wu, X. Liu, Y. Huang, X. Wang, H. Xu, K. Lou and W. Wang, *Chem. Commun.*, 2019, **55**, 7053.
- 16 S. Haubenreisser, T. Wöste, C. Martínez, K. Ishihara and K. Muñoz, *Angew. Chem., Int. Ed.*, 2016, **55**, 1.
- 17 A. Chaudhuri, Y. Venkatesh, B. Jena, K. Behara, M. Mandal and N. Singh, *Org. Biomol. Chem.*, 2019, **17**, 8800.
- 18 K. Tang, M. Chang, T. Lin, H. Pan, T. Fang, K. Chen, W. Hung, Y. Hsu and P. Chou, *J. Am. Chem. Soc.*, 2011, **133**, 17738.
- 19 J. Wu, A. Bi, S. Huang, Y. Li, J. Ding, D. Xiang and W. Zeng, *Chem. Commun.*, 2021, **57**, 801.